Inorg. Chem. **2003**, *42*, 5807–5817

Cu(II)Gly_2HisGly Oxidation by H_2O_2/Ascorbic Acid to the Cu(III) Complex and Its Subsequent Decay to Alkene Peptides

Samantha K. Burke, Yinglin Xu, and Dale W. Margerum*

Department of Chemistry, Purdue University, West Lafayette, Indiana 47907

Received May 27, 2003

Protonation and stability constants for Gly_2HisGly and its Cu(II) complexes (β_{mhl}), determined at 25.0 °C and μ = 0.10 M ($NaClO_4$), have values of log β_{011} = 7.90, log β_{021} = 14.51, log β_{031} = 17.55, log β_{101} = 7.82, log β_{1-21} = –0.80, and log β_{1-31} = –12.7 (where the subscripts refer to the number of metal ions, protons, and ligands, respectively). The reaction of $Cu^{II}(H_{-2}Gly_2HisGly)^-$ with L-ascorbic acid and H_2O_2 at p[H^+] 6.6 rapidly generates $Cu^{III}(H_{-2}Gly_2HisGly)$ with λ_{max} at 260 and 396 nm, which is separated chromatographically. The Cu(III) complex decomposes to give alkene peptide isomers of glycylglycyl-α,β-dehydrohistidylglycine that are separated chromatographically and characterized. These alkene peptide species are present as geometric isomers with imidazole tautomers that have distinct spectral and chemical characteristics. The proposed major isomeric form (94%), *Z*-N^{τ}–H, has a hydrogen on the τ nitrogen of the imidazole ring and three conjugated double bonds. It has absorption bands at 295 and 360 nm at p[H^+] 6.6 in the absence of copper. The proposed minor isomeric form (6%) is *E*-N^{π}–H with a hydrogen on the π nitrogen of the imidazole ring. This isomer has four conjugated double bonds and strongly binds Cu(II) to give a complex with intense absorption bands at 434 and 460 nm.

Introduction

Dervan and co-workers[1,2] coupled the carboxylate end of glycylglycyl-L-histidine to the glycylamine terminal of Hin recombinase, which selectively binds DNA. The addition of Cu(II) followed by H_2O_2 and ascorbic acid led to site-specific oxidative DNA degradation. The ability of Cu(II) or Cu(III) complexes of the tetrapeptide residue glycylglycyl-L-histidylglycine (Gly_2HisGly) to assist in the oxidative degradation and site-specific cleavage of DNA[1−3] is of considerable interest.

Other investigators[4] have proposed that hydroxyl radicals are generated in the reaction of Cu(II)Gly_2HisGly with ascorbic acid and H_2O_2 in a Fenton type mechanism, where Cu(II) is reduced to Cu(I) that reacts with H_2O_2 to generate $^{\bullet}$OH. However, $^{\bullet}$OH is a highly diffusible oxidizing species that would not explain the observed cleavage. Although the intermediate that causes DNA cleavage has not been identified, the limited range of cleavage[1] suggests that it is a nondiffusible oxidant. Therefore, the reactive nature of the oxidizing species and the precision of the DNA degradation implies that the species may be trivalent copper.[3]

Margerum and co-workers have investigated and characterized the Cu(II) and Cu(III) complexes of various peptides with respect to their reactivity,[5−9] structures,[9,10] and products.[5,6] Copper(III) complexes of histidine-containing tripeptides[5] and tetrapeptides[6] undergo rapid oxidative degradation of the peptide. These peptides are oxidized at the third residue to give α-hydroxyhistidyl derivatives that dehydrate to produce alkene species (α,β-dehydrohistidyl derivatives). Decomposition products of histidine-containing copper complexes have been characterized previously by X-ray crystal-

* To whom correspondence should be addressed. E-mail: margerum@purdue.edu.

(1) Mack, D. P.; Iverson, B. L.; Dervan, P. B. *J. Am. Chem. Soc*. **1988**, *110*, 7572−7574.
(2) Dervan, P. B. *Nature* **1992**, *359*, 87−88.
(3) Dervan, P. B. Sequence Specific Recognition and Cleavage of Double Helical DNA. *Proc. Robert A. Welch Found. Conf. Chem. Res., XXXI, Design of Enzymes and Enzyme Models*; The Welch Foundation: Houston, TX; November 2−4, 1987; pp 93−109.
(4) Ueda, J.-I.; Shimatu, Y.; Ozawa, T. *Free Radical Biol. Med*. **1995**, *18*, 929−933.
(5) McDonald, M. R.; Scheper, W. M.; Lee, H. D.; Margerum, D. W. *Inorg. Chem.* **1995**, *34*, 229−237.
(6) McDonald, M. R.; Fredericks, F. C.; Margerum, D. W. *Inorg. Chem.* **1997**, *36*, 3119−3124.
(7) Hamburg, A. W.; Nemeth, M. T.; Margerum, D. W. *Inorg. Chem.* **1983**, *22*, 3535−3544.
(8) Neubecker, T. A.; Kirksey, S. T., Jr.; Chellappa, K. L.; Margerum, D. W. *Inorg. Chem.* **1979**, *18*, 444−448.
(9) Diaddario, L. L.; Robinson, W. R.; Margerum, D. W. *Inorg. Chem.* **1983**, *22*, 1449−1456.
(10) Bal, W.; Djuran, M. I.; Margerum, D. W.; Gray, E. T., Jr.; Mazid, M. A.; Tom, R. T.; Nieboer, E.; Sadler, P. J. *J. Chem. Soc., Chem. Commun.* **1994**, 1889−1890.

10.1021/ic0345774 CCC: $25.00
Published on Web 08/27/2003

lography, where Cu^{II}(glycylglycyl-α,β-dehydrohistamine) crystals were isolated from a solution that originally contained $Cu^{II}(H_{-2}Gly_2His)^-$ in the presence of air.[11,12] If copper(II) were removed from this structure, the resulting alkene peptide would be in a *Z* geometric conformation.[13]

The redox behavior of the copper−peptide complexes in solution may differ significantly from their behavior when attached to Hin recombinase bound to the minor groove of DNA. In addition to changes of the outer-sphere environment, the bound copper complexes are not free to react with one another as they do in solution. In all of our Cu(III) studies where the peptide is oxidized, the initial first-order Cu(III) oxidation step is followed by a rapid reaction with a second Cu(III) complex in order to give stable two electron oxidation products.[5,6,14−18] This cannot occur in the DNA experiments; thus, the isolated Cu(III) species or its initial intermediates would have more time to react with DNA.

In the present work, the Cu(II) complexes of the tetrapeptide are characterized in terms of their stability constants as well as UV−vis and circular dichroic (CD) spectra. Hydrogen peroxide is ineffective in oxidizing Cu(II)−peptide complexes to Cu(III), and ascorbic acid is known to reduce Cu(III) complexes[19] as well as H_2O_2.[20−24] Thus, we were skeptical about the ability of the mixture of H_2O_2 and ascorbic acid to form Cu(III)−peptide complexes. However, we show that Cu(III) complexes are indeed generated from this mixture. Hence, Cu(III) could be an intermediate in the oxidative degradation and cleavage of DNA under Dervan's conditions.[1,2] Under our conditions, the Cu(III) complexes decompose to give relatively stable alkene peptides that are present in several isomeric and tautomeric forms with intense UV−vis spectral bands.

Experimental Section

Reagents. All solutions were prepared with doubly deionized distilled water (18 MΩ), filtered through 0.22 μm filter paper, and stored at 10 °C when not in use. Solutions of NaOH were prepared from a saturated solution, stored under argon, and standardized titrimetrically with potassium hydrogen phthalate. Solutions of $HClO_4$ were standardized with the NaOH. The ionic strength (μ) of each solution was controlled with $NaClO_4$. Solutions of $NaClO_4$ were prepared from the recrystallized salt, gravimetrically standardized, and stored under argon.

Solutions of $Cu(ClO_4)_2$ were prepared from the twice-recrystallized salt and standardized with EDTA. The Gly_2-L-HisGly, Gly_2-L-His, and Gly_4 peptides were purchased from BACHEM Bioscience, while Gly_2-L-$HisNH_2$ and Gly_2Ha were synthesized by Dr. Hsiu-Pu D. Lee at Purdue University. The aqueous Cu(II)−ligand complex was prepared by dissolving 5−10% excess of the peptide with $Cu(ClO_4)_2$ to ensure formation of 1:1 complexes. Phosphate buffer (NaH_2PO_4/Na_2HPO_4 mixtures) was added and the pH adjusted to greater than 6.0 to give complete formation of the complex.

Chemical oxidation of Cu(II)−peptide complexes was achieved by two methods: (1) Cu(II)−peptide species were mixed with H_2O_2 and L-ascorbic acid (H_2A), or (2) Cu(II)−peptide species were mixed with $IrCl_6^{2-}$ where $Na_2(IrCl_6)\cdot 6H_2O$ was standardized spectrophotometrically ($\epsilon_{487} = 4075\ M^{-1}\ cm^{-1}$).[25] H_2O_2 was standardized with $KMnO_4$. L-Ascorbic acid and dehydroascorbic acid (stored in the dark at −8 °C) were used as received. All metal−peptide oxidation reactions were performed under red lights.

Instrumentation and Methodology. Potentiometric titrations (in triplicate) were performed with an Orion model SA 720 research pH meter with a Corning combination glass electrode. The base titrant (0.1 M NaOH) was delivered from a calibrated Gilmont ultra precision micrometer syringe. The solutions were thermostated at 25.0(1) °C and purged with argon during titration. Electrode calibration allowed for correction from measured pH values to $-\log[H^+]$ in order to obtain accurate $[H^+]$ values expressed in molarities. Titration data were analyzed by a modified version[26] of the SCOGS program.

Kinetic studies of fast reactions were performed with an Applied Photophysics model SX-18MV stopped-flow spectrophotometer in a 0.962 cm observation cell. Reaction species were followed at 360 and 528 nm with time scales from 0.1 to 1000 s at 25.0(1) °C and $\mu = 0.10$ M ($NaClO_4$). All rate constants reported are the average of five pushes. SigmaPlot 2001[27] (ver. 7.101) was used for regression analyses. UV−vis absorption spectra were measured with a Perkin-Elmer Lambda 9 UV−vis−NIR spectrophotometer. Spectra were acquired from 200 to 800 nm at 480 nm/min with 120 s intervals between scans. Circular dichroic (CD) spectra were taken with a Jasco J600 spectropolarimeter.

Cyclic voltammetry (CV) and Osteryoung square-wave voltammetry (OSWV) data were collected with a BAS-100 electrochemical analyzer. A glassy carbon working electrode (3 mm diameter), platinum wire auxiliary electrode, and Vycor tip Ag/AgCl reference electrode stored in 3 M NaCl ($E° = 0.194$ V vs NHE) were used.

Cu(II)−peptide complexes were electrochemically oxidized by using a BAS-100 electrochemical analyzer. Solutions of $Cu^{II}(H_{-2}Gly_2HisGly)^-$ at $p[H^+]$ 6.6 were passed through a flow-through bulk electrolysis column[8] to generate $Cu^{III}(H_{-2}Gly_2HisGly)$; $E° = 0.978$ V versus NHE for this couple.[6] The working electrode was a graphite powder electrode packed to a height of 1.3 cm in a porous glass tube (0.5 cm (i.d.)) and wrapped externally with a platinum wire (auxiliary electrode). The reference electrode was a Vycor tip

(11) de Meester, P.; Hodgson, D. J. *J. Am. Chem. Soc.* **1976**, *98*, 7086−7087.
(12) de Meester, P.; Hodgson, D. J. *Inorg. Chem.* **1978**, *17*, 440−444.
(13) IUPAC Commission on the Nomenclature of Organic Chemistry. *Nomenclature of Organic Chemistry: Sections A, B, C, D, E, F, and H*, 1979 ed.; Rigaudy, J., Klesney, S. P., Eds.; Pergamon Press: New York; 1979; pp 476−478.
(14) Hamburg, A. W.; Margerum, D. W. *Inorg. Chem.* **1983**, *22*, 3884−3893.
(15) Margerum, D. W. *Pure Appl. Chem.* **1983**, *55*, 23−34.
(16) Kurtz, J. L.; Burce, G. L.; Margerum, D. W. *Inorg. Chem.* **1978**, *17*, 2454−2460.
(17) Kirksey, S. T., Jr.; Margerum, D. W. *Inorg. Chem.* **1979**, *18*, 966−970.
(18) Rybka, J. S.; Kurtz, J. L.; Neubecker, T. A.; Margerum, D. W. *Inorg. Chem.* **1980**, *19*, 2791−2796.
(19) Margerum, D. W.; Wong, L. F.; Bossu, F. P.; Chellappa, K. L.; Czarnecki, J. J.; Kirksey, S. T.; Neubecker, T. A. In *Bioinorganic Chemistry-II*; Raymond, K. N., Ed.; Advances in Chemistry Series 162, American Chemical Society: Washington, DC, 1977; pp 281−303.
(20) Hand, D. B.; Greisen, E. C. *J. Am. Chem. Soc.* **1942**, *64*, 358−361.
(21) Zambonin, C. G.; Losito, I. *Anal. Chem.* **1997**, *69*, 4113−4119.
(22) Martell, A. E. In *Ascorbic Acid: Chemistry, Metabolism, and Uses*; Seib, P. A., Tolbert, B. M., Eds.; Advances in Chemistry Series 200; American Chemical Society: Washington, DC, 1982, pp 153−178.
(23) Kahn, M. M. T.; Martell, A. E. *J. Am. Chem. Soc.* **1967**, *89*, 4176−4185.
(24) Torreilles, J.; Guerin, M.-C.; Carles, C.; Crastes de Paulet, A. *Bull. Soc. Chim. Fr.* **1989**, *4*, 489−492.
(25) Owens, G. D.; Margerum, D. W. *Inorg. Chem.* **1981**, *20*, 1446−1453.
(26) Hauer, H.; Billo, E. J.; Margerum, D. W. *J. Am. Chem. Soc.* **1971**, *93*, 4173−4178.
(27) *SigmaPlot v. 2001 for Windows*; SPSS, INC.: Chicago, IL, 2001.

Ag/AgCl electrode stored in 3 M NaCl ($E° = 0.194$ V vs NHE). Potentials of 0.8−1.0 V versus Ag/AgCl were applied to the column. A Harvard Apparatus Compact Infusion Multi-fit syringe pump generated flow through the column at a rate of 1−3 mL/min. The column was conditioned with water (100 mL at 1.0 mL/min) and 0.10 M $HClO_4$ (100 mL at 1.0 mL/min). The Cu(III)−peptide complex was collected in dilute $HClO_4$ after preparation in order to limit its decay. However, when p[H$^+$] 7 was necessary, the solution was collected in phosphate buffer.

Reaction intermediates and products were separated by using a Varian 5000 liquid chromatograph equipped with a Hewlett-Packard 1050 diode array detector, with a 1 cm cell path length and 13 μL volume. Whatman Partisil 10 strong cation exchange (SCX) columns were used for separations: analytical (4.6 mm (i.d.) × 250 mm), Magnum 9 (9.4 mm (i.d.) × 250 mm), and Magnum 20 (22 mm (i.d.) × 500 mm). Mobile phases of 0.075 M $[PO_4]_T$ (μ = 0.10 M ($NaClO_4$)) at p[H$^+$] 2.47, 0.037 M $[PO_4]_T$ at p[H$^+$] 6.73, or 0.025 M $(NH_4)HCO_2$ at p[H$^+$] 2.93 were used for separations (flow rate = 1.0−3.0 mL/min, injection volume = 0.050, 0.50, or 5.0 mL, 0.01−5 mM oxidized peptide per injection, and λ_{det} = 220, 360, 402, 434, and 460 nm). All solutions were degassed and filtered before injection. Fractions were collected in iced containers (5 °C) and immediately lyophilized or taken for mass spectrometric analysis. A Virtis FreezeMobile 12 lyophilized samples at −60 °C and 60 millitorr.

Separation of the *E*-N$^\pi$−H conjugated histidyl tautomer from Cu(II) was achieved by collecting 50 fractions of the tautomer (3−5% of 1 mM [Gly$_2$HisGly]$_i$), still bound to Cu(II) at p[H$^+$] 2.47. The p[H$^+$] was increased to 6.5−6.8 and mixed with 200% excess EDTA for 2 h. The resulting mixture was separated chromatographically with 0.037 M $[PO_4]_T$ at p[H$^+$] 6.73, where the Cu(II)−EDTA complex was removed from the unbound tautomer. Separation of geometric isomers of conjugated histidyl tautomers was performed with 0.037 M $[PO_4]_T$ at p[H$^+$] 6.73.

Mass spectrometric data were collected on a Bioion 20R plasma desorption mass spectrometer (PD-MS). Samples were applied to nitrocellulose, and spectra were obtained for 15 min. Electrospray ionization mass spectrometry data were collected by using a Finnigan MAT LCQ mass spectrometer system. The sample was dissolved in water/acetonitrile, and the drying gas was N_2.

IR data were obtained with a Perkin-Elmer Spectrum 2000 FT-IR. The alkene samples were mulled, or a thin film was applied to Teflon tape. Fractions of the alkene products (100 fractions) were collected, lyophilized, and resuspended in D_2O (99.9%) for NMR analysis. ^{1}H NMR spectra were obtained with a Brucker DXR 500 MHz spectrometer for 0.01−0.03 M samples of the alkene peptides run for 500 transients.

Results and Discussion

The generalized cumulative formation reactions of peptide ligands with protons and Cu(II) are given in eq 1, where L$^-$ is the basic form of the ligand, and the stability constant β_{mhl} is defined by eq 2. Analysis of titration data for the peptide ligands in the absence of Cu(II) gives the cumulative protonation constants for amine, imidazole, and carboxylate groups, respectively (eqs 3−5). Three titrations at 25.0 °C and μ = 0.10 M ($NaClO_4$) with 70−100 sets of data each were evaluated with $[L]_T$ = 6.93 mM. Table 1 gives the average value and standard deviation for the β_{011}, β_{021}, and β_{031} constants.

Table 1. Cumulative Protonation and Cu(II) Stability Constants

constant	Gly$_2$HisGly[a]	Gly$_2$His[b]	Gly$_2$His[c]
logβ_{011}	7.90(1)	8.14	8.23
logβ_{021}	14.51(3)	15.06	15.22
logβ_{031}	17.55(5)	17.89	18.06
logβ_{121}		16.72	
logβ_{111}		11.78	13.56
logβ_{101}	7.82(9)	7.55	
logβ_{1-11}		2.68	
logβ_{1-21}	−0.8(1)	−1.92	−1.25
logβ_{1-31}	−12.7(2)		−11.94
logβ_{122}		25.81	
logβ_{112}		20.64	
logβ_{102}		16.68	
logβ_{1-12}		9.73	
logβ_{1-22}		1.43	

[a] This work: 25.0(1) °C, μ = 0.10 M ($NaClO_4$). For ligand titrations only, $[L]_T$ = 6.93 mM; for ligand + Cu(II) titrations, $[L]_T$ ranges from 5.18 to 7.47 mM and $[Cu(II)]_T$ ranges from 4.69 to 5.37 mM. Results are averages from three ligand titrations and from nine ligand + Cu(II) titrations. Numbers in parentheses represent one standard deviation in the last digit reported. [b] Ref 28, μ = 0.15 M (NaCl), 25 °C. [c] Ref 31, 21 °C.

$$m\mathrm{Cu}^{2+} + h\mathrm{H}^+ + l\mathrm{L}^- \overset{\beta_{mhl}}{\rightleftharpoons} \mathrm{Cu}_m(\mathrm{H}_h\mathrm{L}_l) \quad (1)$$

$$\beta_{mhl} = \frac{[\mathrm{Cu}_m(\mathrm{H}_h\mathrm{L}_l)]}{[\mathrm{Cu}^{2+}]^m[\mathrm{H}^+]^h[\mathrm{L}^-]^l} \quad (2)$$

$$\mathrm{H}^+ + \mathrm{L}^- \overset{\beta_{011}}{\rightleftharpoons} \mathrm{HL} \quad (3)$$

$$2\mathrm{H}^+ + \mathrm{L}^- \overset{\beta_{021}}{\rightleftharpoons} \mathrm{H_2L}^+ \quad (4)$$

$$3\mathrm{H}^+ + \mathrm{L}^- \overset{\beta_{031}}{\rightleftharpoons} \mathrm{H_3L}^{2+} \quad (5)$$

The experimental titration curves for solutions of Cu(II) and Gly$_2$HisGly fit equilibria given in eqs 6−11 but did not require equilibria for $Cu(HL)_2$, $CuHL_2$, $CuH_{-1}L_2$, and $CuH_{-2}L_2$. Nine titration results (3 sets in triplicate) were used. The $[Cu]_T$ ranged from 4.69 to 5.37 mM, and $[L]_T$ ranged from 5.18 to 7.47 mM.

$$\mathrm{Cu}^{2+} + \mathrm{H}^+ + \mathrm{L}^- \overset{\beta_{111}}{\rightleftharpoons} \mathrm{Cu(HL)}^{2+} \quad (6)$$

$$\mathrm{Cu}^{2+} + \mathrm{L}^- \overset{\beta_{101}}{\rightleftharpoons} \mathrm{CuL}^+ \quad (7)$$

$$\mathrm{Cu}^{2+} + \mathrm{L}^- \overset{\beta_{1-11}}{\rightleftharpoons} \mathrm{Cu(H_{-1}L)} + \mathrm{H}^+ \quad (8)$$

$$\mathrm{Cu}^{2+} + \mathrm{L}^- \overset{\beta_{1-21}}{\rightleftharpoons} \mathrm{Cu(H_{-2}L)}^- + 2\mathrm{H}^+ \quad (9)$$

$$\mathrm{Cu}^{2+} + \mathrm{L}^- \overset{\beta_{1-31}}{\rightleftharpoons} \mathrm{Cu(H_{-3}L)}^{2-} + 3\mathrm{H}^+ \quad (10)$$

$$\mathrm{Cu}^{2+} + 2\mathrm{L}^- \overset{\beta_{102}}{\rightleftharpoons} \mathrm{CuL_2} \quad (11)$$

Protonation Constants for Gly$_2$HisGly. The individual protonation constants for the amine, imidazole, and carboxylate groups are given in eqs 12−14. The amine protonation constants for Gly$_2$HisGly are slightly lower than those determined for Gly$_2$His[28−30] and GlyHisGly (Table S1).[31,32] The imidazole and carboxylate protonation constants for

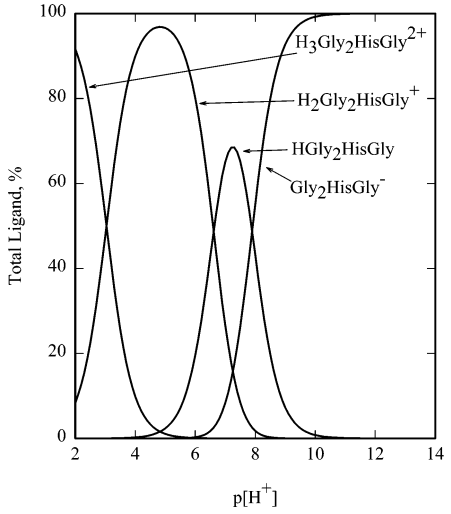

Figure 1. Species distribution diagram for $Gly_2HisGly$, where $[L]_T = [L^-] + [LH] + [LH_2^+] + [LH_3^{2+}] = 6.93$ mM, 25.0(1) °C, and $\mu = 0.10$ M ($NaClO_4$).

$Gly_2HisGly$ and $GlyHisGly$ are different by 0.2−0.4 log units as compared to values for Gly_2His. This suggests that the nearby carboxylate group in the terminal His residue favors the protonation. Figure 1 gives the $Gly_2HisGly$ species distribution as a function of $p[H^+]$.

$$\log K^{NH_3} = \log \beta_{011} = 7.90 \qquad (12)$$

$$\log K^{Im(H)} = \log \beta_{021} - \log \beta_{011} = 6.62 \qquad (13)$$

$$\log K^{COOH} = \log \beta_{031} - \log \beta_{021} = 3.04 \qquad (14)$$

Cu(II)−Ligand Stability Constants. Under our experimental conditions (10−39% excess ligand and 4.67−5.37 mM Cu(II)), no evidence of bis-ligand complexes of $Gly_2HisGly$ with Cu(II) was found. As shown in Table 1, Lau and Sarkar[28,29] reported five bis complexes for Cu(II) and Gly_2His. However, Aiba, Yokoyama, and Tanaka,[30,31] who used only 1:1 reactants, did not report any bis complexes with Gly_2His. In the present work, nine titrations with three different ratios of Cu/L were used to verify the best model for the $Gly_2HisGly$ system. Values were obtained for β_{101}, β_{1-21}, and β_{1-31}, but the data did not fit equilibria corresponding to β_{121}, β_{111}, β_{1-11}, or any bis complexes. The main complex present from pH 5 to 10 is $Cu^{II}(H_{-2}Gly_2HisGly)^-$. Its structure is given in Figure 2a, and the species distribution for all the Cu(II) complexes as a function of $p[H^+]$ is given in Figure 3. The present work found $\log \beta_{1-21} = -0.8$ for $Gly_2HisGly$, which is a factor of $10^{0.45}-10^{1.12}$ more stable than the corresponding complex of Gly_2His.[28,31]

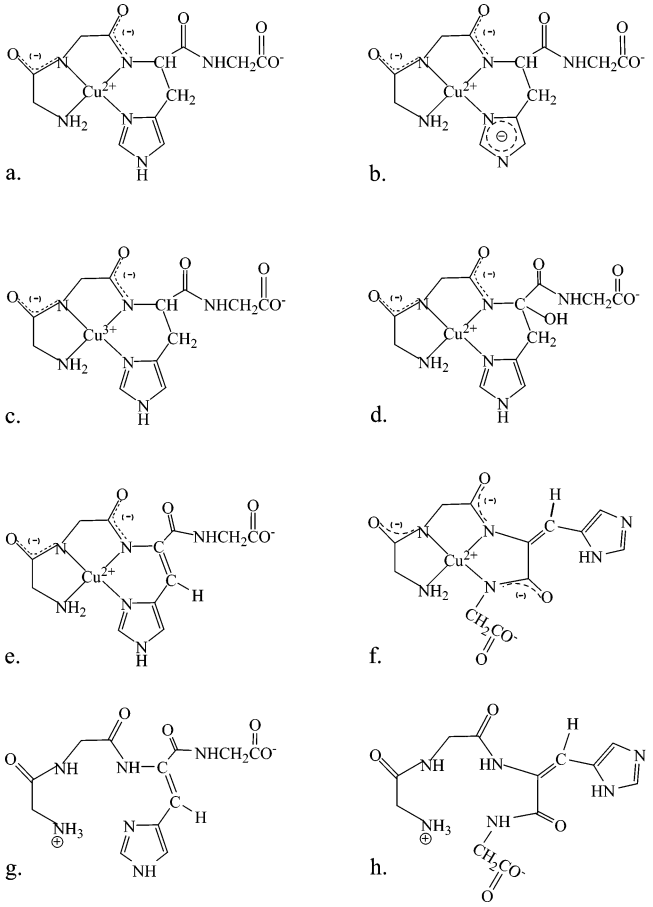

Figure 2. Proposed structures for (a) $Cu^{II}(H_{-2}Gly_2HisGly)^-$, (b) $Cu^{II}(H_{-3}Gly_2HisGly)^{2-}$, (c) $Cu^{III}(H_{-2}Gly_2HisGly)$, (d) $Cu^{II}(H_{-2}Gly_2$-α-OH−$HisGly)^-$, (e) $Cu^{II}(H_{-2}Gly_2$-*Z*-α,β-dehydro(N^{τ}-H)$HisGly)^-$, (f) $Cu^{II}(H_{-3}$-Gly_2-*E*-α,β-dehydro(N^{π}-H)$HisGly)^{2-}$, and glycylglycyl-α,β-dehydrohistidylglycine isomers, (g) *Z*-N^{τ}−H and (h) *E*-N^{π}−H.

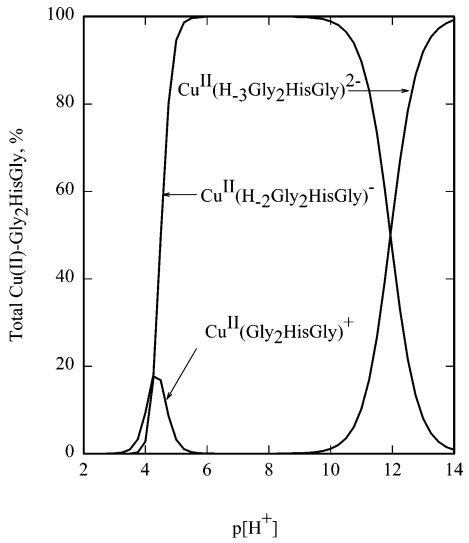

Figure 3. Species distribution diagram for Cu(II)-complexes. $[Cu(II)]_T = 5.14$ mM, $[L]_T = 5.65$ mM, 25.0(1) °C, and $\mu = 0.10$ M ($NaClO_4$). Calculated from potentiometric data.

Small amounts of $Cu^{II}(Gly_2HisGly)^+$ are found at pH 4−5, where Cu(II) is coordinated to an amine nitrogen and imidazolium nitrogen. Above pH 12, $Cu^{II}(H_{-3}Gly_2HisGly)^{2-}$ becomes the main complex, where imidazole deprotonation occurs as shown in Figure 2b.[33] The $Cu^{II}(H_{-3}L)^{2-}$ complex

(28) Lau, S.-J.; Sarkar, B. *J. Chem. Soc., Dalton Trans.* **1981**, *2*, 491−494.
(29) Lau, S.-J.; Kruck, T. P. A.; Sarkar, B. *J. Biol. Chem.* **1974**, *249*, 5878−5884.
(30) Yokoyama, A.; Aiba, H.; Tanaka, H. *Bull. Chem. Soc. Jpn.* **1974**, *47*, 112−117.
(31) Aiba, H.; Yokoyama, A.; Tanaka, H. *Bull. Chem. Soc. Jpn.* **1974**, *47*, 1437−1441.
(32) Bryce, G. F.; Roeske, R. W.; Gurd, F. R. N. *J. Biol. Chem.* **1965**, *240*, 3837−3846.

Table 2. Molar Absorptivity Values for Reaction Intermediates and Products

reaction species	λ, nm	ϵ, M^{-1} cm^{-1}
$Cu^{II}(H_{-2}Gly_2HisGly)^-$	528[a]	96
$Cu^{III}(H_{-2}Gly_2HisGly)$	260[a,b]	4200
	396[a,b]	1700
	360	600
	528	7
$Cu^{II}(H_{-3}Gly_2$-*E*-α,β-dehydro(N^{π}−H)HisGly$)^{2-}$	434[a,b]	7800
	460[a,b]	11,000
	360	1800
	528	160
$Cu^{II}(H_{-2}Gly_2$-*Z*-α,β-dehydro(N^{τ}−H)HisGly$)^-$	295[a]	1000
	360[a]	2900
	460	230
	528	134
Gly_2-*Z*-α,β-dehydro(N^{τ}−H)$HisGly^{2+}$	285[b]	1700
	350[b]	2300

[a] λ_{max} for p[H^+] 6.6. [b] λ_{max} for p[H^+] 2.47.

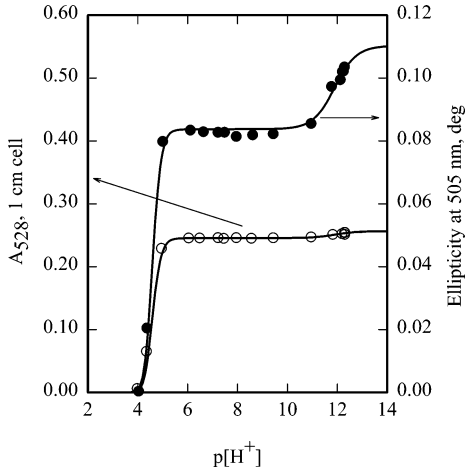

Figure 4. Dependence of the absorbance at 528 nm (A_{528}) and the ellipticity at 505 nm (θ_{505}) of Cu(II)−Gly_2HisGly complexes on p[H^+]. $[Cu(II)]_T$ = 2.55 mM, $[L]_T$ = 2.82 mM, μ = 0.10 M ($NaClO_4$), and 0.1 dm cell. Both fits are calculated from potentiometrically determined values.

is characteristic of other histidine/histamine-containing tripeptide complexes of Cu(II) in which imidazole deprotonation takes place.[31,34] The pK_a^{Im} value of 11.9 in $Cu^{II}(H_{-3}Gly_2$-$HisGly)^{2-}$ is in contrast to values greater than 14 for histidine itself.[35]

Spectral Characteristics of Cu(II)Gly_2HisGly Complexes. UV−vis spectra of $Cu^{II}(H_{-2}Gly_2HisGly)^-$ and $Cu^{II}(H_{-3}Gly_2HisGly)^{2-}$ have λ_{max} at 528 nm with molar absorptivities (Table 2) of 96 and 100 M^{-1} cm^{-1}, respectively. Previous investigators[4] found the same λ_{max} value for $Cu^{II}(H_{-2}Gly_2HisGly)^-$ but did not report its molar absorptivity. Absorbance data at 528 nm with increasing p[H^+] from 4 to 10 agreed with the potentiometrically determined constants. Figure 4 shows these absorbance values and circular dichroic data from p[H^+] 4 to 12.3. These data demonstrate evidence for the loss of a proton from the imidazole portion of His (Figure 2b) with a pK_a = 11.9. The CD spectra of the Cu(II) complexes of Gly_2HisGly have one negative band at 590 nm and two positive bands centered at 305 and 505 nm, where the specific ellipticity ($[\psi] = \theta/cl$, c = concentration in g/mL and l = cell length in dm) at 505 nm is 811(6) and 1068(8) deg·mL/dm·g for $Cu^{II}(H_{-2}Gly_2$-$HisGly)^-$ and $Cu^{II}(H_{-3}Gly_2HisGly)^{2-}$, respectively.

Lack of Oxidation of $Cu^{II}(H_{-2}Gly_2HisGly)^-$ by O_2 or H_2O_2. Oxidation of $Cu^{II}(H_{-2}Gly_2HisGly)^-$ to Cu(III)[6] by H_2O_2[36] is thermodynamically favorable (by 0.307 V at p[H^+] 6.6 and 25.0 °C). However, no spectral changes were observed up to 15 h when excess H_2O_2 (50 mM) was added to $Cu^{II}(H_{-2}Gly_2HisGly)^-$ solutions at p[H^+] 6.6. Similarly, solutions of the Cu(II) complex saturated with either O_2 or air show no change for at least 10 h. On the other hand, $Cu^{II}(H_{-3}Gly_4)^{2-}$ is readily oxidized to $Cu^{III}(H_{-3}Gly_4)^-$ by oxygen,[37] which may be due to the 0.348 V lower reduction potential for $Cu^{III/II}(H_{-3}Gly_4)^{-/2-}$ compared to $Cu^{III/II}(H_{-2}$-$Gly_2HisGly)^{0/-}$. In the work by Dervan et al.,[1] DNA cleavage was observed within 100 min after complexing Cu(II) to Gly_2HisGly residues of modified Hin recombinase and adding H_2O_2 and ascorbic acid in phosphate buffer. If $Cu^{III}(H_{-2}Gly_2HisGly)$ is a possible intermediate that leads to site-specific DNA degradation, H_2O_2/ascorbic acid mixtures are necessary to initiate cleavage within 100 min.

Lack of Reduction of $Cu^{II}(H_{-2}Gly_2HisGly)^-$ by Ascorbic Acid. Ascorbic acid is well-known as a powerful reducing agent.[38] The primary species present at p[H^+] 6.6 is ascorbate (HA^-) because H_2A has pK_a values of 4.03 and 11.34.[39] An electrode potential of 0.185 V (vs NHE) at pH 7 and 21 °C has been determined for ascorbic acid.[40] In the presence of trace metal ions, H_2A is easily oxidized by O_2 to give dehydroascorbic acid (A) and H_2O_2.[22,23,41−43] In our work, H_2A oxidation by O_2 in the presence of trace Cu(II) (10^{-6} M) gave a k_{obsd} value of 1.51(8) × 10^{-4} s^{-1}, which suggests that significant amounts of H_2O_2 are not produced in the reaction and that O_2 will not affect the oxidation reaction of Cu(II)Gly_2HisGly with H_2O_2/H_2A. On the other hand, Buettner[44] shows that the loss of ascorbate in air-saturated and metal-free solutions at pH 7 has a first-order rate constant of less than 6 × 10^{-7} s^{-1}. Hydrogen peroxide does not appear to react directly with ascorbic acid,[20,21] but H_2A oxidation by H_2O_2 is strongly catalyzed by Cu(II), Fe(III), or histidine.[22−24] The UV absorption band for HA^- at

(33) Tesfai, T. M.; Margerum, D. W. Submitted for publication.
(34) Gajda, T.; Henry, B.; Aubry, A.; Delpuech, J. J. *Inorg. Chem.* **1996**, *35*, 586−593.
(35) (a) Walba, H.; Isensee, R. *J. Am. Chem. Soc.* **1955**, *77*, 5488−5492. (b) George, P.; Hanania, G. I. H.; Irvine, D. H.; Abu-Issa, I. *J. Chem. Soc.* **1964**, 5689−5694. (c) Yagil, G. *Tetrahedron* **1967**, *23*, 2855−2861.
(36) *Standard Potentials in Aqueous Solution*; Bard, A. J., Parsons, R., Joseph, J., Eds.; Marcel Dekker: New York; 1985; pp 57−58.
(37) Kurtz, J. L.; Burce, G. L.; Margerum, D. W. *Inorg. Chem.* **1978**, *17*, 2454−2460.
(38) (a) Barron, E. S. G.; DeMeio; Klemperer, F. *J. Biol. Chem.* **1936**, *112*, 625−640. (b) Davies, M. B.; Austin, J.; Partridge, D. A. *Vitamin C: Its Chemistry and Biochemistry*; Royal Society of Chemistry Paperbacks: Cambridge, England, 1991; pp 4−45.
(39) Martell, A. E.; Smith, R. M. *Critical Stability Constants*; Plenum Press: New York; 1977; Vol. 3, p 264.
(40) Erdey, L.; Bodor, E. *Anal. Chem.* **1952**, *24*, 418−420.
(41) Yamazaki, I.; Mason, H. S.; Piette, L. *J. Biol. Chem.* **1960**, *235*, 2444−2449.
(42) Bielski, B. H. In *Ascorbic Acid: Chemistry, Metabolism, and Uses*; Seib, P. A., Tolbert, B. M., Eds.; Advances in Chemistry Series 200; American Chemical Society: Washington, DC, 1982; pp 81−100.
(43) Scarpa, M.; Vianello, F.; Signor, L.; Zennaro, L.; Rigo, A. *Inorg. Chem.* **1996**, *35*, 5201−5206.
(44) Buettner, G. R. *J. Biochem. Biophys. Methods* **1988**, *16*, 27−40.

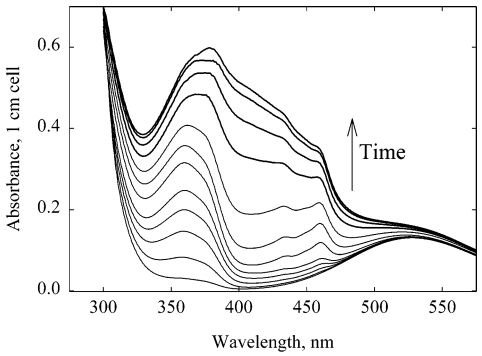

Figure 5. UV−vis spectral changes when $Cu^{II}(H_{-2}Gly_2HisGly)^-$ ($[Cu(II)]_T = 1.36$ mM, $[L]_T = 1.41$ mM) is mixed with ascorbic acid (1.0 mM) and H_2O_2 (1.00 mM) at p[H^+] 6.6 in 0.020 M $[PO_4]_T$, $\mu = 0.10$ M ($NaClO_4$), and 25.0 °C, where time at 360 nm per scan is as follows: (1) 197 s, (2) 317 s, (3) 557 s, (4) 797 s, (5) 917 s, (6) 1037 s, (7) 1157 s, (8) 1277 s, (9) 2177 s, (10) 2357 s, (11) 3317 s, and (12) 5915 s.

265 nm is intense with ϵ values of 14 500[45] or 15 000 M^{-1} cm^{-1}.[43] Our studies indicate that dehydroascorbic acid has an absorption band at 300 nm. However, all these bands are well removed from the 350−475 nm range used in most of the present work.

Ueda and co-workers[4] reported that ascorbic acid reduces $Cu^{II}(H_{-2}Gly_2HisGly)^-$ to its Cu(I) complex. Their conclusion was based on an absorbance loss at 528 nm as the ascorbic acid concentration was increased. However, buffer is needed to prevent ascorbic acid from decreasing the pH with subsequent loss of Cu(II) coordination. Our work shows no loss in absorbance at 528 nm for 1.0 mM $Cu^{II}(H_{-2}Gly_2HisGly)^-$ in 0.5−3.5 mM ascorbic acid at p[H^+] 6.4−6.6. Therefore, Cu(I) is not formed, and without Cu(I), a proposed Fenton type reaction with H_2O_2 would not generate hydroxyl radicals[4] in mixtures of $Cu^{II}(H_{-2}Gly_2HisGly)^-$, ascorbic acid, and H_2O_2.

Oxidation of $Cu^{II}(H_{-2}Gly_2HisGly)^-$ by Ascorbic Acid and H_2O_2 To Form $Cu^{III}(H_{-2}Gly_2HisGly)$. Figure 5 shows the large spectral changes that occur from 275 to 575 nm over a period of 100 min when $Cu^{II}(H_{-2}Gly_2HisGly)^-$ is mixed with H_2O_2 and ascorbic acid at p[H^+] 6.6. Various possible combinations of reactants were mixed and observed for 4 or more hours, and no spectral bands at 360 and 434/460 nm were found unless $Cu^{II}(H_{-2}Gly_2HisGly)^-$, ascorbic acid, and H_2O_2 were all present. The characteristic $Cu^{II}(H_{-2}Gly_2HisGly)^-$ absorption band at 528 nm changes very little, but a large spectral band at 360 nm as well as two smaller bands at 434 and 460 nm grow in. Previous studies by McDonald and co-workers[5,6] show that alkene peptide species, which have absorption bands near 360 nm, serve as excellent indicators of transitory Cu(III)-intermediates. Therefore, the data in Figure 5 indicate the probable presence of a Cu(III)-intermediate in the H_2O_2/H_2A reaction.

Copper(III)−peptide complexes contain two UV−vis absorption bands, one in the vicinity of 250−280 nm and the other at 350−410 nm.[5,6,8] The decomposition reactions of Cu(III) complexes of histidine-containing peptides are general-base assisted, and their rates increase greatly as the p[H^+] increases.[5,6] Decay of Cu(III) in these reactions produces an α-OH intermediate of histidine that rapidly dehydrates to form an alkene peptide.

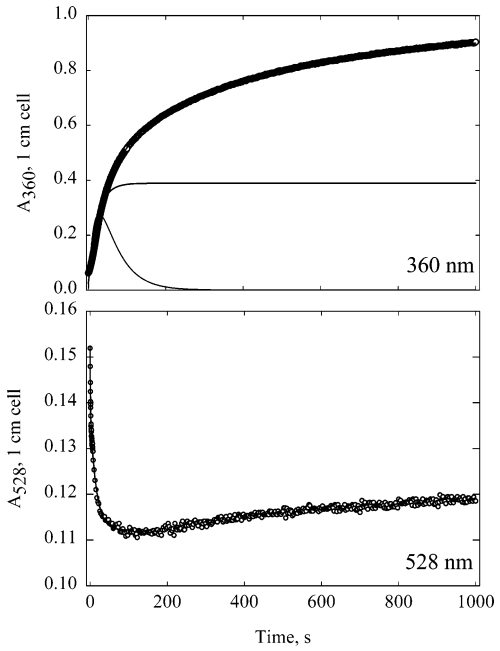

Figure 6. Stopped-flow traces of $Cu^{II}(H_{-2}Gly_2HisGly)^-$ in the presence of ascorbic acid and H_2O_2 at p[H^+] 6.6 at 360 and 528 nm. $[Cu(II)]_T = 1.64$ mM, $[L]_T = 1.72$ mM, $[H_2A] = 1.4$ mM, $[H_2O_2] = 1.37$ mM, $\mu = 0.10$ M ($NaClO_4$), p[H^+] = 6.6 (0.020 M $[PO_4]_T$), 25.0 °C, and 0.962 cm cell. A_{360} shows the formation of Cu(III) and the alkene peptide. A_{528} shows the loss of Cu(II) to give Cu(III), where Cu(III) decays to an α-OH intermediate, and then α-OH dehydrates to the alkene peptide. Because the alkene has a greater ϵ_{528}, no α-OH loss is observed.

Stopped-flow methods permit the partial loss of $Cu^{II}(H_{-2}Gly_2HisGly)^-$ to be observed within 30 s (Figure 6) at 528 nm when it is mixed with H_2O_2/H_2A at p[H^+] 6.6. The initial product, $Cu^{III}(H_{-2}Gly_2HisGly)$, has little absorbance at 528 nm, but its rapid formation can be seen at 360 nm. Subsequent reactions of the Cu(III) complex (60−1000 s) produce alkene peptide species and regenerate some of the initial Cu(II) complex. The alkene species have even larger ϵ_{360} values than Cu(III).

Chromatographic Separation of Cu(III). Direct monitoring of the formation and loss of $Cu^{III}(H_{-2}Gly_2HisGly)$ at its 396 nm absorption maximum proved challenging due to overlapping UV−vis absorption bands from its alkene peptide products. Therefore, separation of the reaction mixture was essential to characterize and identify Cu(III) as an intermediate in the H_2O_2/H_2A reaction. The $Cu^{III}(H_{-2}Gly_2HisGly)$ complex was separated from the reaction mixture ($Cu^{II}(H_{-2}Gly_2HisGly)^-$, H_2O_2, H_2A, and other products) by allowing a reaction time of only 30−50 s at p[H^+] 6.6 prior to its injection on the chromatographic column. A strong cation exchange column was used with 0.075 M $[PO_4]_T$, $\mu = 0.10$ M ($NaClO_4$), and p[H^+] 2.47 as the eluent. The Cu(III) peak that eluted at 3.7 min had characteristic absorption bands at 260 and 396 nm (Figure 7). An electrochemically generated Cu(III) complex gave identical retention times and spectral bands. Table 3 gives the retention times for various species in the reaction mixture. The chromatographic separation of the Cu(III) complex at p[H^+]

(45) Steinman, H. G.; Dawson, C. R. *J. Am. Chem. Soc.* **1942**, *64*, 1212−1219.

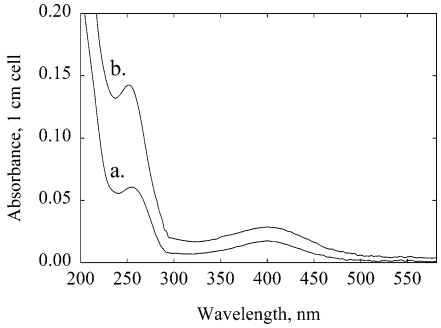

Figure 7. Diode array spectra of $Cu^{III}(H_{-2}Gly_2HisGly)$ complexes eluting at 3.7 min. Elution occurring at p[H^+] = 2.47 in 0.075 M $[PO_4]_T$, λ_{det} = 402 nm, 1 cm cell path length, 1.0 mL/min flow rate, and 500 μL sample loop. (a) Chemically generated Cu(III) species: $[Cu(II)]_T$ = 1.02 mM, $[L]_T$ = 1.12 mM, $[H_2O_2]$ = 1.00 mM, $[H_2A]$ = 1.00 mM, air saturated, μ = 0.10 M ($NaClO_4$), p[H^+] = 6.6 (0.020 M $[PO_4]_T$), and 25.0 °C. (b) Electrochemically generated Cu(III) species: $[Cu(II)]_T$ = 1.03 mM, $[L]_T$ = 1.14 mM, air saturated, μ = 0.10 M ($NaClO_4$), p[H^+] = 6.6 (0.020 M $[PO_4]_T$), 0.82 V vs Ag/AgCl, 2.0 mL/min flow rate, and 25.0 °C. Collected in 0.084 M $HClO_4$.

Table 3. Retention Times of Reaction Species[a]

reaction species	retention time, min
H_2O_2[b]	2.9
L-ascorbic acid[b]	3.3
Cu(III)Gly$_2$HisGly[c]	3.7
dehydroascorbic acid[b]	4.2
Cu(II)−*E*-N$^{\tau}$−H complex[c]	4.7
Cu(II)−H_2PO_4[b]	5.9
Gly$_2$-*Z*-α,*β*-dehydro(N$^{\tau}$−H)HisGly[c]	10.5
Gly$_2$HisGly[b]	15

[a] Whatman Partisil 10 SCX analytical column, 25.0 °C, 0.075 M $[PO_4]_T$, μ = 0.10 M ($NaClO_4$), p[H^+] 2.47, 1 cm cell, 1.0 mL/min flow rate, and HP diode array detector. [b] Retention time was checked against that of a known standard. [c] Retention time was checked against that of electrochemically generated Cu(III) and its decay products.

2.47 is possible because the complex is sluggish in its substitution reactions (as are other Cu(III) complexes)[5,6,8] and remains coordinated at low pH. On the other hand, the original Cu(II) complex dissociates quickly at low pH. Chromatographic separations of the reaction mixture after 50 s demonstrate 89(4)% loss of the original ascorbic acid and 49(2)% loss of H_2O_2.

Copper(III) Yields. The molar absorptivity of the Cu(III) complex (ϵ_{396} = 1.7(2) × 10^3 M^{-1} cm^{-1}) was determined by reaction of the Cu(II) complex with $IrCl_6^{2-}$ with stopped-flow and was confirmed by bulk electrolysis measurements. Chromatographic separation gave Cu(III) yields of 47(2)% and 97(2)% (based on $[Cu(II)]_T$) for chemically and electrochemically generated mixtures. These values were calculated by using the molar absorptivity of the Cu(III)-intermediate after taking into account the decay at p[H^+] 2.5 during the 222 s interval between the mixing and observation times.

When a 2:1 (H_2A/H_2O_2) ratio is used, the yield of Cu(III) is 98% (based on $[Cu(II)]_T$). Higher levels of O_2 in the solution reduce the amount of Cu(III) formed because O_2 also reacts with H_2A. We observe only half of our anticipated yield with a 1:1 (H_2A/H_2O_2) ratio. This is attributed to Cu(II)Gly$_2$HisGly catalysis of reactions between H_2O_2 and H_2A that depletes their concentrations. Nevertheless, in most of the present work, a 1:1 ratio of H_2A and H_2O_2 was maintained to be consistent with Dervan's studies.[1,2]

Reaction Sequence. The proposed series of reactions is given in eqs 15−17 where $Cu^{II}(H_{-2}Gly_2HisGly)^-$ reacts with the ascorbic acid/H_2O_2 mixture to generate $Cu^{III}(H_{-2}Gly_2$-HisGly). Two Cu(III) complexes are needed to oxidize the histidyl residue to an α-hydroxy derivative, Gly$_2$-α-OH−HisGly (eq 16), that in turn decays to form the alkene peptide, Gly$_2$-α,*β*-dehydro-HisGly (eq 17). Copper(III) loss is rapid ($t_{1/2}$ = 32 s at p[H^+] 6.6) to form the α-OH−His derivative. The proposed Cu(II) complex of this derivative is shown in Figure 2d. Similar α-OH intermediates are known to exist for $Ni^{II}(H_{-2}Gly_2$-α-OH−Ha)[10,46] which was identified by X-ray crystallography and for Aib$_2$-α-OH−Ha which was identified by ^{1}H NMR.[5]

$$Cu^{II}(H_{-2}Gly_2HisGly)^- \xrightarrow{H_2O_2/H_2A} Cu^{III}(H_{-2}Gly_2HisGly) \quad (15)$$

$$2Cu^{III}(H_{-2}Gly_2HisGly) \xrightarrow{H_2O} 2H^+ + Cu^{II}(H_{-2}Gly_2HisGly)^- + Cu^{II}(H_{-2}Gly_2\text{-}\alpha\text{-OH-HisGly})^- \quad (16)$$

$$Cu^{II}(H_{-2}Gly_2\text{-}\alpha\text{-OH-HisGly})^- \rightarrow Cu^{II}(H_{-2}Gly_2\text{-}\alpha,\beta\text{-dehydro-HisGly})^- + H_2O \quad (17)$$

The detailed mechanism of Cu(III) formation by the H_2O_2 and ascorbic acid mixture in eq 15 remains uncertain. However, hydroxyl radicals ($E°$ = 1.97 V at p[H^+] 6.6)[47] are proposed to form in H_2A/H_2O_2 oxidation reactions,[24,48] and reaction between $^{\bullet}$OH and $Cu^{II}(H_{-2}Gly_2HisGly)^-$ to give the corresponding Cu(III) complex is favorable by 0.99 V. The $Cu^{III}(H_{-2}Gly_2HisGly)$ complex would be an excellent reservoir for additional redox reactions. In Dervan's method,[1,2] this could lead to site-specific cleavage because the Cu(III) complex is attached to Hin recombinase and is not mobile. In the present case the Cu(III)−peptide complexes are mobile and can react with each other (eq 16) to cause a two electron oxidation of the peptide.

Cu(III) Formation and Decomposition Kinetics. Observed decomposition rate constants for Cu(III) generated by $IrCl_6^{2-}$ or bulk electrolysis were determined by monitoring absorbance loss at its λ_{max} (396 nm). A first-order loss of Cu(III) at 396 nm was found with k_{obsd} = 1.7(2) × 10^{-2} s^{-1} at p[H^+] 6.6 and k_{obsd} = 5.4(2) × 10^{-3} s^{-1} at p[H^+] 2.5. A first-order loss in Cu(III) is observed because the second Cu(III) in eq 16 reacts in a subsequent, rapid step. The loss of electrochemically generated Cu(III) in the presence of 1.0 mM ascorbic acid gave k_{obsd} = 2.5(4) × 10^{-2} s^{-1} at p[H^+] 6.6 and 4.9(4) × 10^{-3} s^{-1} at p[H^+] 2.5. The presence of 1.0 mM H_2A at p[H^+] 6.6 slightly increases Cu(III) loss and suggests that only small amounts of Cu(III) are reduced by ascorbic acid at this concentration. However, higher con-

(46) Sakurai, T.; Nakahara, A. *Inorg. Chim. Acta* **1979**, *34*, L243−L244.
(47) *Standard Potentials in Aqueous Solution*; Bard, A. J., Parsons, R., Joseph, J., Eds.; Marcel Dekker: New York, 1985; p 63.
(48) Oya, Y.; Takenaka, A.; Ochi, T.; Yamamoto, K. *Mutat. Res.* **1992**, *266*, 281−289.

centrations of H_2A (20 mM) rapidly reduce Cu(III) (within 18 s) to the Cu(II)−peptide complex, and less than 2% of the alkene decomposition products (based on $[Cu(III)]_T$) are formed. Lappin and co-workers[49] found that oxidation of ascorbic acid by Ni(IV) complexes is enhanced at pH values near its first pK_a ($pK_a = 4.03$), and they also reported a factor of 4 slower reduction at pH 2.3 compared to pH 5.3.

Rapid formation of Cu(III) by the H_2O_2/H_2A reaction with the Cu(II) complex was followed by stopped-flow methods because the UV−vis data from 200 to 6000 s in Figure 5 are due to the alkene absorption bands after the loss of Cu(III). Two alkene products are identified that are imidazole tautomers and geometric isomers of one another. We assign the major decomposition product at 360 nm (45(2)% based on $[Cu(III)]_T$) as $Cu^{II}(H_{-2}Gly_2$-*Z*-α,*β*-dehydro(N^{τ}−H)HisGly)$^-$ (Figure 2e). The initial Cu(II) and Cu(III) complexes are bound with 5,5,6-membered chelate rings so that after dehydration the alkene peptide must be in a *Z* geometric conformation. As shown in Figure 2e, the imidazole in the Cu(II)−alkene peptide complex must also be in a N^{τ}−H tautomeric form. The major product forms 7 times faster than the minor product, $Cu^{II}(H_{-3}Gly_2$-*E*-α,*β*-dehydro(N^{π}-H)-HisGly)$^{2-}$ (Figure 2f), with absorption bands at 434/460 nm (3−5% based on peptide recoveries). Their identification is discussed later.

In Figure 6, data collected at p[H^+] 6.6 show rapid formation of Cu(III) at 360 nm ($k_{15} = 8.1(3) \times 10^{-2}$ s^{-1}) but do not illustrate the loss of Cu(III) ($k_{16} = 2.14(3) \times 10^{-2}$ s^{-1}) to give the α-OH species because the Cu(II)−*Z*-N^{τ}−H species that grows in with time ($k_{17} = 2.24(3) \times 10^{-3}$ s^{-1}) has a larger extinction coefficient (Table 2). A consecutive first-order mechanism[50] (A → B → C → D) was used to fit the data for the formation of Cu(III) ($\epsilon_{360} = 600$ M^{-1} cm^{-1}), its decay to $Cu^{II}(H_{-2}Gly_2$-α-OH−HisGly)$^-$, and formation of the alkene peptide ($\epsilon_{360} = 2900$ M^{-1} cm^{-1}). The copper(II)−peptide complexes have minimal absorbance at 360 nm ($\epsilon_{360} = 2$ M^{-1} cm^{-1}).

Figure 6 also includes data collected at 528 nm that show loss of $Cu^{II}(H_{-2}Gly_2HisGly)^-$ within 30 s to form Cu(III), which decays (eq 16) to give $Cu^{II}(H_{-2}Gly_2HisGly)^-$ and $Cu^{II}(H_{-2}Gly_2$-α-OH−HisGly)$^-$. Molar absorptivities of 96 M^{-1} cm^{-1} at 528 nm are used for $Cu^{II}(H_{-2}Gly_2HisGly)^-$ and $Cu^{II}(H_{-2}Gly_2$-α-OH−HisGly)$^-$, whereas the Cu(III) complex has $\epsilon_{528} = 7$ M^{-1} cm^{-1}. The rate constants for Cu(III) formation and loss are within the error of the 360 nm data. The initial rate data at 528 nm give a calculated Δ*A* that corresponds to 49% Cu(II) loss (eq 15), but only 24% absorbance loss is observed because of the high molar absorptivity of the subsequent alkene species (Table 2) that form after α-OH dehydration (eq 17).

Formation Rate Constants of Alkene Products. Because only 21% of the Cu(II)−*Z*-N^{τ}−H alkene (based on $[Cu(III)]_T$) is generated within 1000 s (stopped-flow time limit), the reaction was monitored over a longer period with a UV−vis spectrophotometer, and the absorbance increase was fit to a single-exponential curve. This k_{17} value was found to be $1.5(4) \times 10^{-3}$ s^{-1} at p[H^+] 6.6 over the period of 200−6000 s and gave a 44% yield of the Cu(II)−*Z*-N^{τ}−H alkene (based on $[Cu(III)]_T$). Interference from the Cu(II)−*E*-N^{π}−H species at 360 nm is minimal (6% of the total signal).

Observation of the minor alkene product (Cu(II)−*E*-N^{π}−H) was possible because it has intense absorption bands at 434 and 460 nm. Data collected at 460 nm for the formation of the Cu(II)−*E*-N^{π}−H alkene gave an observed rate constant of $2.2(1) \times 10^{-4}$ s^{-1} at p[H^+] 6.6 after 6000 s. The absorbance increase at 460 nm fits a double-exponential curve where $\epsilon_{460} = 11\,000$ M^{-1} cm^{-1} for the Cu(II)−*E*-N^{π}−H species, $\epsilon_{460} = 230$ M^{-1} cm^{-1} for the Cu(II)−*Z*-N^{τ}−H alkene, and $k_{17} = 1.5(4) \times 10^{-3}$ s^{-1} for the Cu(II)−*Z*-N^{τ}−H alkene. The double-exponential fit represents two concurrent pathways: one is the formation of the Cu(II)−*Z*-N^{τ}−H alkene by the α-OH species, and the other is the formation of the Cu(II)−*E*-N^{π}−H alkene from another α-OH species that is partially dissociated from Cu(II). The second α-OH species is proposed to be a transient bis complex that forms by dissociation of the imidazole group of the α-OH species from Cu(II) that is replaced by residual Gly_2HisGly. Bis-ligand Cu(II) complexes were not directly observed in our work, but small amounts of these complexes could be present within our experimental error (Table 1). Dehydration of the α-OH peptide must take place when the imidazole group is not coordinated to copper in order to generate the *E* isomer. The bis complex would facilitate formation of the *E*-N^{π}−H alkene. This process is described in more detail in a later section. The observed rate constant for the formation of the Cu(II)−*E*-N^{π}−H alkene is a combination of the formation of the proposed transient bis complex and its dehydration. An induction period is apparent initially in the reaction but is not included in the fit. The induction period is believed to occur because of dissociation of imidazole from copper and formation of the transient bis complex. The formation of the Cu(II)−*E*-N^{π}−H alkene is 14% slower at p[H^+] 6.6 as compared to the Cu(II)−*Z*-N^{τ}−H species, and its yield is kinetically limited.

Enhanced Cu(II) Complexation by *E*-N^{π}−H. The *Z*-N^{τ}−H alkene dissociates from Cu(II) below pH 3, whereas the *E*-N^{π}−H species remains complexed even at p[H^+] 1.7. The 434/460 nm bands are unaffected by the pH change. Spectral properties of individual reaction species are summarized in Table 2. The proposed minor alkene product (*E*-N^{π}−H) retains Cu(II) strongly and does not release it unless EDTA is present for 2 h at neutral pH. This resulting mixture is chromatographically separated at neutral pH, and the unbound product has bands at 295 and 370 nm. Addition of Cu(II) to the unbound *E*-N^{π}−H species regenerates the 434/460 nm peaks. The *Z*-N^{τ}−H copper complex has a significantly lower λ_{max} than the *E*-N^{π}−H copper complex, which indicates that different groups are coordinated to Cu(II). Voltammetric data show a much lower reduction potential (by 0.29 V) for the Cu(III/II)−*E*-N^{π}−H species ($E' = 0.946$

(49) Lappin, A. G.; Laranjeira, M. C. M.; Lawson, Y.-O. *J. Chem. Soc., Dalton Trans.* **1981**, 721−725.

(50) (a) Espenson, J. H. *Chemical Kinetics and Reaction Mechanisms*, 2nd ed.; McGraw-Hill: New York, 1995; pp 70−90. (b) Connors, K. A. *Chemical Kinetics: The Study of Reaction Rates in Solution*; VCH Publishers: New York, 1990; pp 61−77.

V (vs NHE) at p[H^+] 6.7)[51] as compared to the Cu(III/II)−*Z*-N$^\tau$−H complex. The 0.29 V lower reduction potential supports a triply deprotonated structure where the deprotonated peptide nitrogens are strong σ-donors to copper and will lower the potential by ∼0.3 V.[52] Removal of a proton from the third peptide nitrogen is attributed to the extended conjugation of the *E*-N$^\pi$−H isomeric form. Thus, the *E*-N$^\pi$−H isomeric form (Figure 2f) appears to coordinate Cu(II) strongly and in a different conformation than the *Z*-N$^\tau$−H species. Mass spectrometric analysis demonstrates isotopic splitting consistent with copper for chromatographically separated fractions of the Cu(II)−*E*-N$^\pi$−H complex.

Gly_2-α-OH-HisGly Dissociation Permits *E*-N$^\pi$−H Formation. The major reaction product (*Z*-N$^\tau$−H) forms when the α-OH intermediate is bound to Cu(II) in a 5,5,6-membered ring system (Figure 2). The minor product (*E*-N$^\pi$−H) must form when Gly_2-α-OH-HisGly is either fully or partially dissociated from Cu(II) (without imidazole coordination) and the histidyl residue can freely rotate. We have measured the rate constant for formation of the Cu(II)−peptide complex (8.8×10^2 M^{-1} s^{-1} at p[H^+] 6.8) and estimated a dissociation rate constant of 7×10^{-7} s^{-1} at p[H^+] 6.6. This would correspond to only 0.4% complete dissociation in 6000 s. Therefore, partial dissociation must provide the main pathway for the formation of the *E* isomer. Proton-assisted partial dissociation of imidazole in Gly_2His from Cu(II) has been observed[53,54] and would have a rate constant of 0.045 s^{-1} at p[H^+] 6.6. The partially dissociated intermediate would have a very small concentration. The 5−10% excess of Gly_2HisGly in solution could assist this reaction by forming small amounts of a bis complex. Under our conditions (p[H^+] 6.6 and 0.020 M $[PO_4]_T$), 99.3% copper is bound and 0.7% additional Gly_2HisGly is available for coordination. The bis complex could aid the full dissociation of the α-OH peptide, or it could hinder reformation of the imidazole−Cu(II) bond long enough for dehydration to occur. The bis complex would not be expected to be in equilibrium with the α-OH species because the terminal glycyl group provides steric hindrance. Other researchers have reported bis-ligand complexes for Gly_2His,[28,55] where small amounts of these species would be present under our conditions.

After dehydration occurs, we propose that increased electron delocalization in the conjugated peptide helps to deprotonate the third peptide nitrogen with the assistance of copper. Copper binds the *E*-N$^\pi$−H alkene in a 5,5,5-membered ring system (Figure 2f). This type of ring formation also is observed with copper−tetraglycine complexes.[8,52,56,57] The pK_a of the third peptide nitrogen is 9.14 for Gly_4 in the presence of Cu(II)[56] but is orders of magnitude lower for the conjugated peptide. The imidazole group of Gly_2-α-OH-HisGly protonates when it is no longer bound to Cu(II). The imidazolium nitrogen pK_a values are decreased due to conjugation, and intramolecular hydrogen bonding from the hydrogen on the N$^\pi$ to the terminal glycyl residue[58] would favor deprotonation of the N$^\tau$. The greater conjugation of the *E*-N$^\pi$−H isomer is more thermodynamically stable than the *E*-N$^\tau$−H form. A 5,5,7-membered chelate, where the N$^\tau$ coordinates copper instead of the third peptide nitrogen, is not possible because of steric hindrance. The minor alkene occurs after Cu(III) forms and decays (within 100 s, Cu(III) formation $t_{1/2}$ is 8.5 s and decay $t_{1/2}$ is 32 s) and the α-OH species becomes partially dissociated ($t_{1/2}$ = 15 s). Then, dehydration and deprotonation of the third peptide nitrogen would form this complex. The 100 min time frame is sufficient to allow for all these processes to occur.

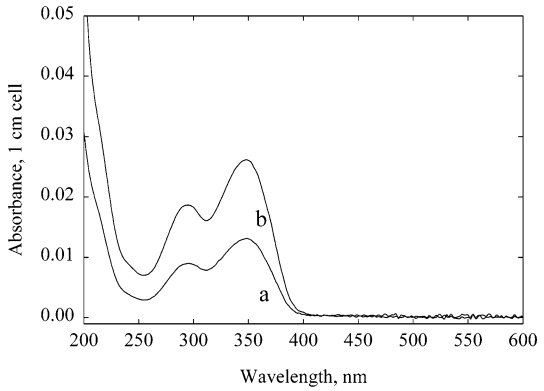

Figure 8. Diode array spectra of Gly_2-*Z*-α,β-dehydro(N$^\tau$−H)HisGly eluting at 10.5 min. Elution occurring at p[H^+] = 2.47 in 0.075 M $[PO_4]_T$, λ_{det} = 360 nm, 1 cm cell path length, 1.0 mL/min flow rate, and 500 μL sample loop. (a) Chemically generated alkene species: $[Cu(II)]_T$ = 1.02 mM, $[L]_T$ = 1.12 mM, $[H_2O_2]$ = 1.00 mM, $[H_2A]$ = 1.00 mM, air saturated, μ = 0.10 M ($NaClO_4$), p[H^+] = 6.6 (0.020 M $[PO_4]_T$), and 25.0 °C. (b) Electrochemically generated alkene species: $[Cu(II)]_T$ = 1.03 mM, $[L]_T$ = 1.14 mM, air saturated, μ = 0.10 M ($NaClO_4$), p[H^+] = 6.6 (0.020 M $[PO_4]_T$), 0.82 V vs Ag/AgCl, 1.0 mL/min flow rate, and 25.0 °C. Collected in 0.084 M $HClO_4$.

Chromatographic Separation of Alkene Products. Copper(III) decomposition products generated from the H_2O_2/H_2A reaction were separated on a strong cation exchange column at p[H^+] 2.47 and 0.075 M $[PO_4]_T$ (μ = 0.10 M ($NaClO_4$)). Elution at 10.5 min gave a species with absorption bands at 285 and 350 nm (Figure 8), while the peak eluting at 4.7 min had a diode array spectrum (Figure 9) with bands at 434 and 460 nm. The species with spectral bands at 434/460 nm is the Cu(II)−*E*-N$^\pi$−H alkene, and the species with peaks at 285/350 nm is the *Z*-N$^\tau$−H alkene. Electrochemically generated Cu(III) decomposition products gave identical retention times and spectral bands, which further supports the presence of Cu(III) in the H_2O_2/H_2A reaction. Elution of the *Z*-N$^\tau$−H alkene corresponds to a retention time when unbound to Cu(II) (average charge is +1.6), which is a function of its imidazolium nitrogen pK_a values (p$K_a^{Im(H)}$ = 3.7(1) and pK_a^{Im} = 8.4(1)).[51] The parent peptide, Gly_2HisGly,

(51) Burke, S. K.; Killingbeck, L. E.; Margerum, D. W. Alkene Peptide Geometric Isomers with Imidazole Tautomers of Gly_2-α,β-dehydro-HisGly. To be submitted for publication.
(52) Bossu, F. P.; Chellappa, K. L.; Margerum, D. W. *J. Am. Chem. Soc.* **1977**, *99*, 2195−2203.
(53) Cooper, J. C.; Wong, L. F.; Venezky, D. L.; Margerum, D. W. *J. Am. Chem. Soc.* **1974**, *96*, 7560−7562.
(54) Wong, L. F.; Cooper, J. C.; Margerum, D. W. *J. Am. Chem. Soc.* **1976**, *98*, 7268−7274.
(55) Sakurai, T.; Nakahara, A. *Inorg. Chem.* **1980**, *19*, 847−853.
(56) Youngblood, M. P.; Chellappa, K. L.; Bannister, C. E.; Margerum, D. W. *Inorg. Chem.* **1981**, *20*, 1742−1747.
(57) Margerum, D. W.; Chellappa, K. L.; Bossu, F. P.; Burce, G. L. *J. Am. Chem. Soc.* **1975**, *97*, 6894−6896.
(58) Steiner, T.; Koellner, G. *Chem. Commun.* **1997**, 1207−1208.

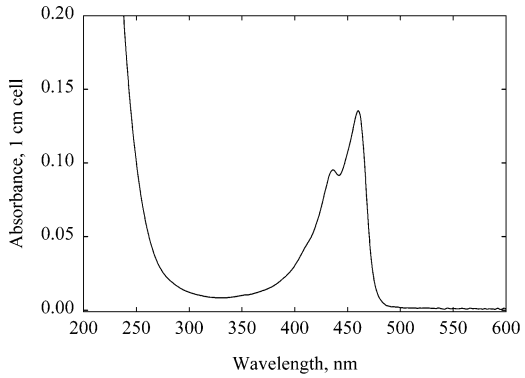

Figure 9. Diode array spectrum of Cu(II) bound to Gly_2-*E*-α,β-dehydro-(N^{π}−H)HisGly eluting at 4.7 min. Elution occurring at p[H^+] = 2.47 in 0.075 M $[PO_4]_T$, λ_{det} = 360 nm, 1.0 mL/min flow rate, 1 cm cell path length, and 5.0 mL sample loop. Chemically generated alkene species: $[Cu(II)]_T$ = 1.02 mM, $[L]_T$ = 1.12 mM, $[H_2O_2]$ = 1.00 mM, $[H_2A]$ = 1.00 mM, air saturated, μ = 0.10 M ($NaClO_4$), p[H^+] = 6.6 (0.020 M $[PO_4]_T$), and 25.0 °C.

begins to elute a minute later because it has a slightly more positive charge (average charge is +1.7) at the elution pH due to its different degree of imidazole protonation. The Cu(II) complexes of the *Z*-N^{τ}−H alkene and Gly_2HisGly are destroyed upon acidification to p[H^+] 2.47. In acid, the ligand adds a second proton to imidazole, and there are no longer tautomeric forms. When the p[H^+] is adjusted to 6.7, it is possible to separate the *Z*-N^{τ}−H and *Z*-N^{π}−H isomers.[51] Only the *Z*-N^{τ}−H isomer forms a strong Cu(II) complex.

The *E*-N^{π}−H alkene has imidazole pK_a values lower by 3−6 log units than Gly_2HisGly because conjugation in the oxidized peptide delocalizes the electron density and reduces protonation. The *E*-N^{π}−H alkene remains bound to Cu(II) at the elution p[H^+] of 2.47. The 434/460 nm absorption bands disappear to give 295/370 nm absorption bands when the solution is mixed with EDTA for 2 h and chromatographically separated. Addition of Cu(II) to the pure *E*-N^{π}−H fraction regenerates the 434/460 nm bands. This species has an earlier retention time (average charge is −0.5) than the *Z*-N^{τ}−H alkene and Gly_2HisGly that is a function of its imidazole pK_a values ($pK_a^{Im(H)}$ = 2.2(8) and pK_a^{Im} = 7.1(6)) and copper binding.[51]

Maximum alkene yields were obtained after allowing the products to form for 100 min at p[H^+] 6.6. Yields for the chemically and electrochemically generated *Z*-N^{τ}−H alkene are 45(2)% and 47(1)% (based on $[Cu(III)]_T$), respectively. The Cu(II)−*E*-N^{π}−H species is a minor product of the reaction and has a yield of 3−5%, based on Gly_2HisGly (49(1)%) and *Z*-N^{τ}−H recoveries, which accounts for the remaining oxidized peptide. The reaction sequence in eq 16 predicts 50% recovery of Gly_2HisGly. The molar absorptivity for the Cu(II)−*E*-N^{π}−H species was estimated from its yield (Table 2).

Identification of Cu(III) Decomposition Products. Fractions of Cu(III) decay products were collected and analyzed by mass spectrometry, ^{1}H NMR, and IR. Mass spectrometric data (PD-MS and ESI-MS) for both products gave a peak at *m*/*z* = 325.4. This value represents loss of two hydrogens from the original peptide to give Gly_2-α,β-dehydro-HisGly $(M + H)^+$. The other peaks in the spectra are sodium adducts or hydrolysis products.[51] The fraction collected at 4.7 min gave a *m*/*z* of 387.2, demonstrating that the *E*-N^{π}−H species is still bound to Cu(II) because of an isotope splitting consistent with copper $(Cu(II) + M + e^-)^+$. Copper complexes were not observed in mass spectrometric data for the *Z*-N^{τ}−H fraction. ^{1}H NMR analysis of the *Z*-N^{τ}−H and *E*-N^{π}−H alkenes without the metal present gave a singlet at δ = 5.9 and 6.2 ppm that indicates both species contain a double bond between the C^{α} and C^{β}. Two singlets at δ = 7.0/8.3 and 7.1/8.4 ppm, which are characteristic of protons on the imidazole carbons, were observed for the *Z*-N^{τ}−H and *E*-N^{π}−H species. The greater downfield shift for the protons of the *E*-N^{π}−H alkene compared to the *Z*-N^{τ}−H species demonstrates a more conjugated system. FT-IR data also illustrated the presence of a conjugated system of double bonds in the oxidized peptide structure because of the sharp C=C stretch observed at 1620−1630 cm^{-1}. Therefore, both species are alkenes with a conjugated system of double bonds, and the *E*-N^{π}−H alkene has more conjugation than the *Z*-N^{τ}−H species and retains Cu(II) at low pH.

The absorption bands for both alkene peptides are pH dependent.[51] A typical spectrum of the alkene peptide species under acidic conditions is observed with two λ_{max} values at 285 and 350 nm, as in Figure 8. Both alkene species have these bands at low pH when unbound to Cu(II).[51] At neutral pH, the *Z*-N^{τ}−H alkene has λ_{max} at 295 and 360 nm, while the *E*-N^{π}−H alkene has λ_{max} at 295 and 370 nm when not coordinated to Cu(II). At high pH, both species have peaks at 305 and 400 nm, which represent the fully deprotonated forms. The spectral bands for the *E*-N^{π}−H alkene have a slightly higher λ_{max} that indicates a more delocalized structure because of the fourth bond in direct conjugation (Figure 2f). The spectral characteristics suggest greater conjugation for the *E*-N^{π}−H alkene and are in agreement with the ^{1}H NMR data. Therefore, the two alkenes were assigned as imidazole tautomers of one another in which the *E*-N^{π}−H alkene has a N^{π}-H assignment because it has four double bonds in conjugation and the *Z*-N^{τ}−H species has a N^{τ}−H assignment because it has three double bonds in conjugation, as seen in Figure 2e. Tautomers of L-histidine found in proteins and small peptides have been previously described in the literature,[58−70] and they are observed to coexist at neutral pH with reported ratios of 8:2[59,60] or 6.5:3.5[61] (N^{τ}−H/N^{π}−H).

(59) Ashikawa, I.; Itoh, K. *Chem. Lett.* **1978**, 681−684.
(60) Tanokura, M. *Biochim. Biophys. Acta* **1983**, *742*, 586−596.
(61) Farr-Jones, S.; Wong, W. Y. L.; Gutheil, W. G.; Bachovchin, W. W. *J. Am. Chem. Soc.* **1993**, *115*, 6813−6819.
(62) Giralt, E.; Ludevid, M.-D.; Pedroso, E. *Bioinorg. Chem.* **1986**, *14*, 405−416.
(63) Aubry, A.; Vlassi, M.; Marraud, M. *Int. J. Pept. Protein Res.* **1986**, *28*, 637−648.
(64) Shimba, N.; Takahashi, H.; Sakakura, M.; Fujii, I.; Shimba, I. *J. Am. Chem. Soc.* **1998**, *120*, 10988−10989.
(65) Tanokura, M. *Biochim. Biophys. Acta* **1983**, *742*, 576−585.
(66) Munowitz, M.; Bachovchin, W. W.; Herzfeld, J.; Dobson, C. M.; Griffin, R. G. *J. Am. Chem. Soc.* **1982**, *104*, 1192−1196.
(67) Jewsbury, P.; Kitagawa, T. *Biophys. J.* **1994**, *67*, 2236−2250.
(68) Bhattacharya, S.; Sukits, S. F.; MacLaughlin, K. L.; Lecomte, J. T. L. *Biophys. J.* **1997**, *73*, 3230−3240.
(69) Reynolds, W. F.; Peat, I. R.; Freedman, M. H.; Lyerla, J. R., Jr. *J. Am. Chem. Soc.* **1973**, *95*, 328−331.

We do not observe any interconversion between the *Z* and *E* alkene products, but their respective imidazole tautomers do interconvert with pH alteration.[51] Because we obtain geometric isomers and imidazole tautomers of Gly$_2$-α,*β*-dehydro-HisGly with different degrees of protonation, 16 possible species result in which 4 isomeric forms of the alkene are present at neutral pH.[51] In other systems, imidazole tautomer interconversion is too rapid to observe,[71] but conjugation within the peptide freezes the tautomer forms and eliminates their interconversion at neutral pH. The *Z*-N$^{\pi}$−H and *E*-N$^{\tau}$−H species result only when the solution pH becomes acidic and causes protonation of both imidazolium nitrogens. After the alkene peptide is fully protonated, the solution pH is increased to neutral pH, and a ratio of both imidazole tautomers is observed.[51] The same effect holds for the reverse situation in which the solution pH is made basic (imidazole fully deprotonated) and then decreased to neutral pH. Fractions of the four neutral isomer species (*Z*-N$^{\tau}$−H, *E*-N$^{\pi}$−H, *Z*-N$^{\pi}$−H, and *E*-N$^{\tau}$−H) were collected, and peaks at 434 and 460 nm were only present when copper was added to the pure *E*-N$^{\pi}$−H fraction. The N$^{\pi}$−H isomer forms have a 10 nm greater λ_{max} than the N$^{\tau}$−H species.

The imidazole tautomer assignments are based on their absorption bands, imidazolium pK_a values, elution characteristics, and ^{1}H NMR, while the geometric isomer assignments were based on reduction potentials, enhanced copper binding, and interconvertibility. This work shows that tautomer species can be distinguished because they are slow to interconvert due to the presence of a conjugated system of double bonds. Crystal structure data by de Meester and Hodgson[11,12] show an alkene peptide species (Cu^{II}(H$_{-2}$Gly$_2$-α,*β*-dehydro-Ha)) that is present as a *cis* isomer (*Z* isomer).

Acknowledgment. This work was supported by National Science Foundation Grants CHE-98-18214 and CHE-0139876. Also, we are grateful to Hsiu-Pu D. Lee for the syntheses of the tripeptide amide, Gly$_2$-L-HisNH$_2$.

Supporting Information Available: Tables and figures with supplemental kinetic and product data. This material is available free of charge via the Internet at http://pubs.acs.org.

IC0345774

(70) Blomberg, F.; Maurer, W.; Rüterjans, H. *J. Am. Chem. Soc.* **1977**, *99*, 8149−8159.
(71) Toullec, J. *Adv. Phys. Org. Chem.* **1982**, *18*, 1−77.